Proceedings of Science and Mathematics
Faculty of Science, Universiti Teknologi Malaysia
Vol. 14, 2022, page 125-132

Enhancement of Photoelectrochemical Water Splitting by ZnO Nanorods as Photosensitive Anode

M. S. Salleh[a,b], M. S. Aziz[a,b]*, G. Krishnan[a,b], N. Mufti[c], M. F. Omar[b], S. Daud[a,b], F. D. Ismail[b], M. D. H. Wirzal[d], U. Niaz[e]

[a] Laser Centre, Ibnu Sina Institute for Scientific and Industrial Research, Universiti Teknologi Malaysia (UTM), 81310 Skudai, Johor, Malaysia

[b] Department of Physics, Faculty of Science, Universiti Teknologi Malaysia (UTM), 81310 Skudai, Johor, Malaysia

[c] Department of Physics, Faculty of Mathematics and Natural Sciences, State University of Malang (UM), Jl. Semarang 5, Malang, 65145, Indonesia

[d] Centre of Research in Ionic Liquids, Universiti Teknologi Petronas (UTP), 32610 Seri Iskandar, Perak, Malaysia

[e] Department of Physics, University of Education, 54770 Lahore, Pakistan

*Corresponding author: safwanaziz@utm.my

Abstract

The fabrication of zinc oxide (ZnO) thin films and nanorods on fluorine-doped tin oxide (FTO) substrate as an effective and reliable photoanode material for photoelectrochemical (PEC) water splitting has received very much of attention recently. Using non-vacuum spray pyrolysis and sol-gel immersion method, an improved fabrication approach to generate homogenous nanorods (106 to 163 nm in diameter) has been demonstrated. X-ray diffraction (XRD), scanning electron microscope (SEM) and field emission scanning electron microscope (FESEM), Energy Disperse X-ray (EDX), UV-Visible spectrometer, and linear sweep voltammetry analysis were used to investigate the impact of nanostructure on the conductivity, charge carrier concentration, optical, and PEC properties of ZnO thin film and nanorods. With a preferred orientation around the (002) plane, the hexagonal wurtzite structure was confirmed by XRD and FESEM to be present in ZnO nanorods. It has been experimentally demonstrated that ZnO nanorods improved photocurrent (1.3 mA/cm^2) with an external bias voltage of 1.0 V_{SCE} under light irradiation as suggested by the photoelectrochemical and transient photocurrent studies. Overall, ZnO in its nanostructure form showed better performances than its ZnO thin film counterpart in photoelectrochemical water splitting as photosensitive anode.

Keywords: ZnO; thin film; nanorods; water splitting;

Introduction

As a result of the current difficulty with the availability of energy, the global demand for energy has become a significant concern on a global scale (Hsieh et al., 2020). In order to solve the lack of non-renewable energy sources, researchers have been looking into sustainable, distinctive, and original techniques (Inayat et al., 2020). Furthermore, they also have made a big effort to look into sustainable, safe, and clean energy sources (Joy et al., 2018). Since water is a plentiful and available source of hydrogen, PEC water splitting is recognised as a practical method for converting solar energy to green hydrogen (Acar & Dincer, 2014). Among the numerous initiatives to produce green hydrogen, PEC water splitting has produced superior outcomes to other techniques (Liu et al., 2016).

ZnO has been proposed as an excellent option to function as a photoanode of PEC since it is an n-type semiconductor with a similar bandgap energy to TiO_2 but greater absorption efficiency across a wide range of the solar spectrum (Dong et al., 2014; Ong et al., 2018). Additionally, it is environmentally friendly, has a high exciton binding energy of 60 MeV, and a high electron transport mobility of 115 to 155 cm^2.V^{-1}.s^{-1} (Hassanpour et al., 2017; Liu et al., 2016). Researchers have been actively examining ZnO for its unique morphology and crystallinity characteristics due of its relatively rich morphological world and crystalline structure (Hassanpour et al., 2017; Kang et al., 2015). In addition, ZnO is a biocompatible material that is abundant in nature, non-toxic, and has a strong piezoelectricity (Hassanpour et al., 2017). The potential uses of ZnO-based nanorods, nanowires, nanotubes, and

nanowhiskers in electronics and optoelectronics have recently attracted attention (Nandi et al., 2016). Due to its high crystallinity, which offers efficient carrier routes in comparison to thin-film based structures, ZnO nanorods have been extensively investigated for applications in light emission, field emission, field effect transistors, sensors, and solar cells (Nandi & Major, 2017). This study examines the performance of ZnO thin films and nanorods as photoanode in PEC water splitting synthesized via spray pyrolysis and the sol-gel immersion method on FTO substrates.

Materials and methods

In order to fabricate ZnO thin film on a FTO substrate, a straightforward spray pyrolysis process was used to create a thin layer of ZnO. The substrates were extensively cleaned using an ultrasonic cleaning method at 50 °C for 30 minutes in hot water, deionized water, and a mixture of acetone and iso-propyl alcohol. As the precursor of the ZnO, zinc nitrate hexahydrate was dissolved in deionized water to create an aqueous solution of 0.25M. The substrate was first heated to 350 °C and maintained at the temperature. After that, 5 mL of the zinc nitrate hexahydrate aqueous solution was sprayed over the FTO substrate to deposit 5 layers of ZnO thin film over the course of 30 minutes. The thin coating was then dried on a hotplate for 20 minutes at 200 °C. Sol-gel immersion method was used to develop ZnO seed layer into nanorods. Hexamethylenetetramine solution and zinc nitrate hexahydrate solution were combined and submerged in an ultrasonic bath for 30 minutes at 50 °C. The solution is then aged and agitated on an ultrasonic stirrer for three hours. The solution was then put into a Schott bottle, which had a layer of face-up ZnO seeds at the bottom. After that, the bottle was submerged in 95 °C water for 4 hours. Following these procedures, the samples were washed with deionized water and dried for 10 minutes on a hotplate at 150 °C.

Shimadzu XRD by $CuK\alpha_1$ monochromator radiation source with (λ = 0.154 Å) at 30 mA and around 40kV was used to analyse the structural characteristics of both ZnO thin films and nanorods. In order to disclose the crystal structure of the nanorods film, spectra were recorded in 2° increments. In order to ascertain the elemental composition of Zn and O in the manufactured thin film and nanorods, Hitachi TM3000 EDX was used, together with SEM in investigating the surface morphology of the ZnO thin films. Meanwhile, the morphology of ZnO nanorods was examined using a Hitachi SU8020 FESEM. In order to investigate the optical properties of the samples, UV-Vis diffuse absorbance spectra were plotted to estimate the absorption via UV-3600 Plus Series Spectrometer. The measured wavelengths were between 300 and 800 nm, and the outcomes were then analytically modelled. Using the Tauc plot, the energy bandgaps of the samples were determined from the absorption spectra.

Furthermore, the photoelectrochemical investigations were carried out in 1.0 M NaOH aqueous solution utilising a three-electrode arrangement, with manufactured nanorods serving as the working electrode and a standard calomel electrode (SCE) serving as the reference electrode, as shown in Figure 1. Dark and lit currents were measured using a potentiostat (Dropsens) with a UV light at a scan rate of 0.01.

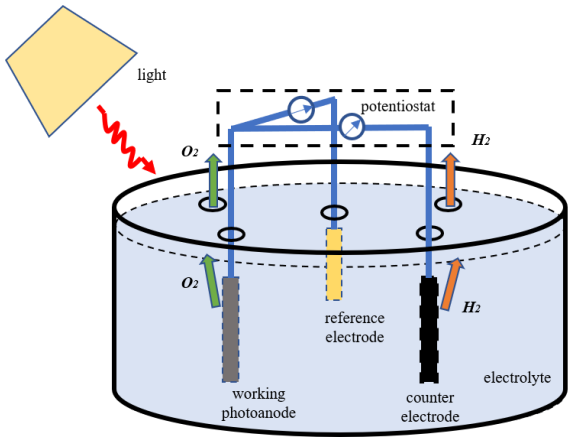

Figure 1 PEC water splitting system with three-electrode configuration setup

Results and discussion

The XRD patterns of the ZnO thin film and nanorod photoanode, which correspond to JCPDS# 36-1451, are shown in Figure 2. At 2θ = 31.83° (100), 34.51° (002), 36.31° (101), 47.59° (102), 56.62° (110), 62.98° (103), 66.41° (200), 67.94° (112), and 69.08° (201), sharp diffraction peaks can be seen for both patterns. In contrast to ZnO thin film, where peak (101) at 36.31° is the highest, while peak (002) of ZnO nanorods at 34.51° became the highest peak. This is because of the nanorods were grown at c-axis from a thin film seed layer (Mamat et al., 2011). Furthermore, the ZnO nanorods' predominant phase was hexagonal wurtzite ZnO crystal structure.

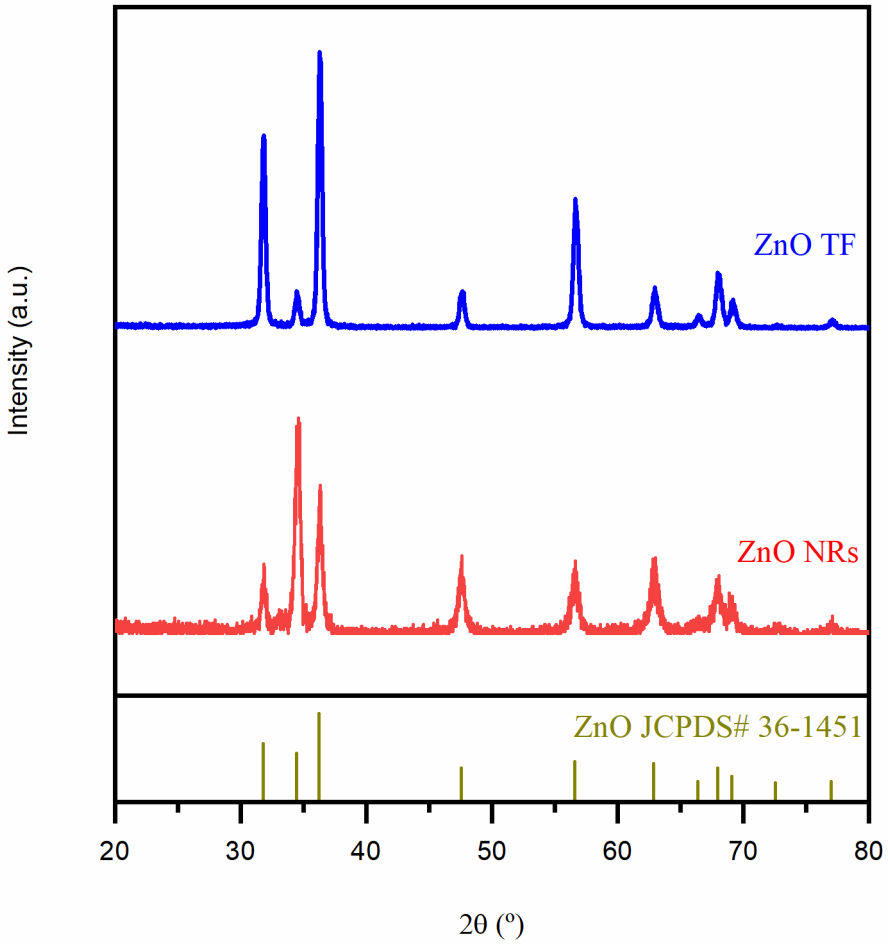

Figure 2 XRD patterns of ZnO thin film and ZnO nanorods.

The well-known Debye-Scherrer formula is used to analyse the average crystallite size (D) of these ZnO thin films and nanorods, as Equation 1(Ocakoglu et al., 2015):

$$D = \frac{k\lambda}{\beta cos\theta} \quad (1)$$

Where k is the crystallite shape factor (0.94), β is the observed angular FWHM of the highest peak, λ is the X-ray wavelength (1.5406A° for Cu Ka_1) and θ is the Bragg's angle. Average crystallite size of all samples is shown in Table 1.

Table 1: Information of average crystallite size calculation for ZnO thin films and ZnO nanorods photoanode

Sample	β (°)	β (rad)	2θ (°)	θ (°)	D (nm)
ZnO TF	0.4686	0.0082	36.31	18.155	185.8579
ZnO NRs	0.5354	0.0093	34.51	17.255	163.0550

The surface morphology of a thin ZnO sheet is shown in Figure 3. Figure 3(a) shows the successfully generated uniform and smooth thin film on the substrate. Figure 3(b) shows that when the magnification is increased to 10k, thin film grains in the shape of needles can be observed being manufactured on top of the substrate. This is due to nanowires have begun to grow from the seed layer (Safwan et al., 2022). Meanwhile, Figure 3(c) and (d) of the FESEM micrographs of the ZnO nanorods photoanode demonstrate that the nanorods growth were laterally the vertical c-axis. The figure's hexagonal form demonstrated that rods have a wurtzite hexagonal ZnO crystal structure (Gu et al., 2020).

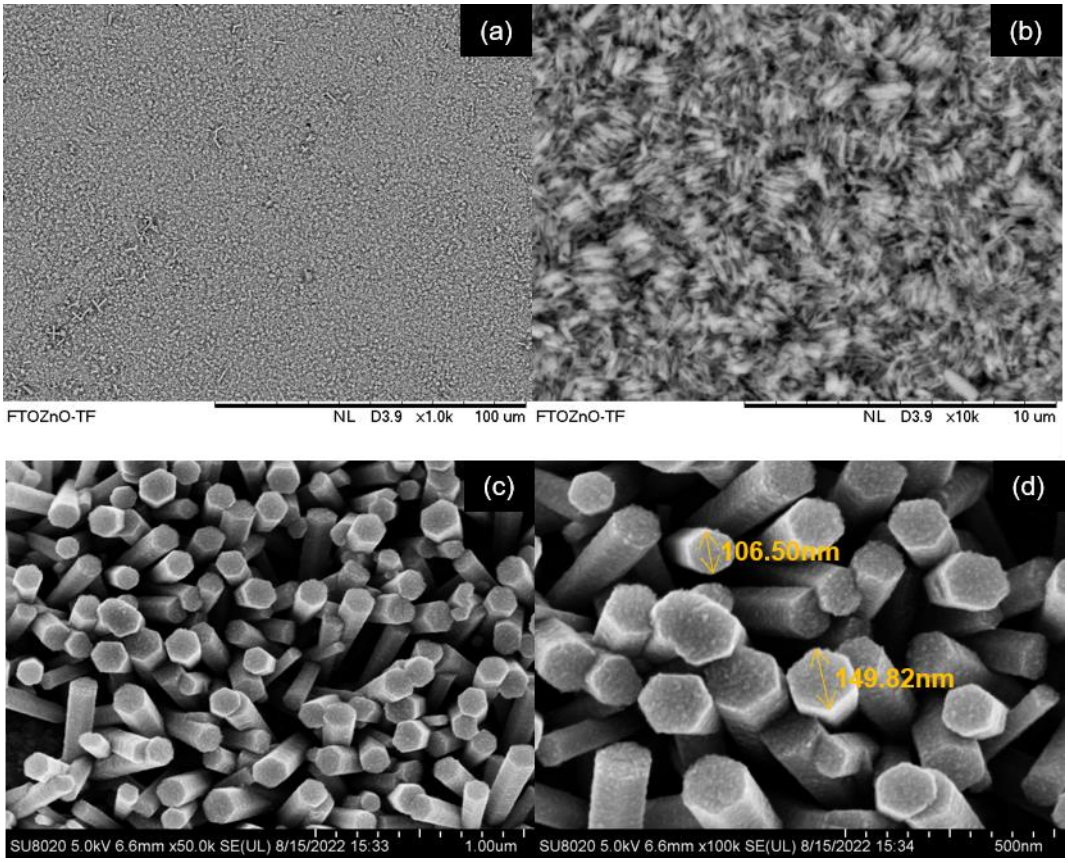

Figure 3 SEM micrographs of ZnO thin film at (a) 1k and (b) 10k magnification; FESEM micrographs of ZnO nanorods at (c) 50k and (d) 100k magnification

Figure 4 shows the normal EDX peaks of Zn and O; no other elements' impurity peaks were seen. This proves that no contamination was occurred during the fabrication of both samples. In Table 2, the atomic percentages and relative weights of the ZnO thin film and nanorod photoanode are comparable, following the chemical formula for ZnO.

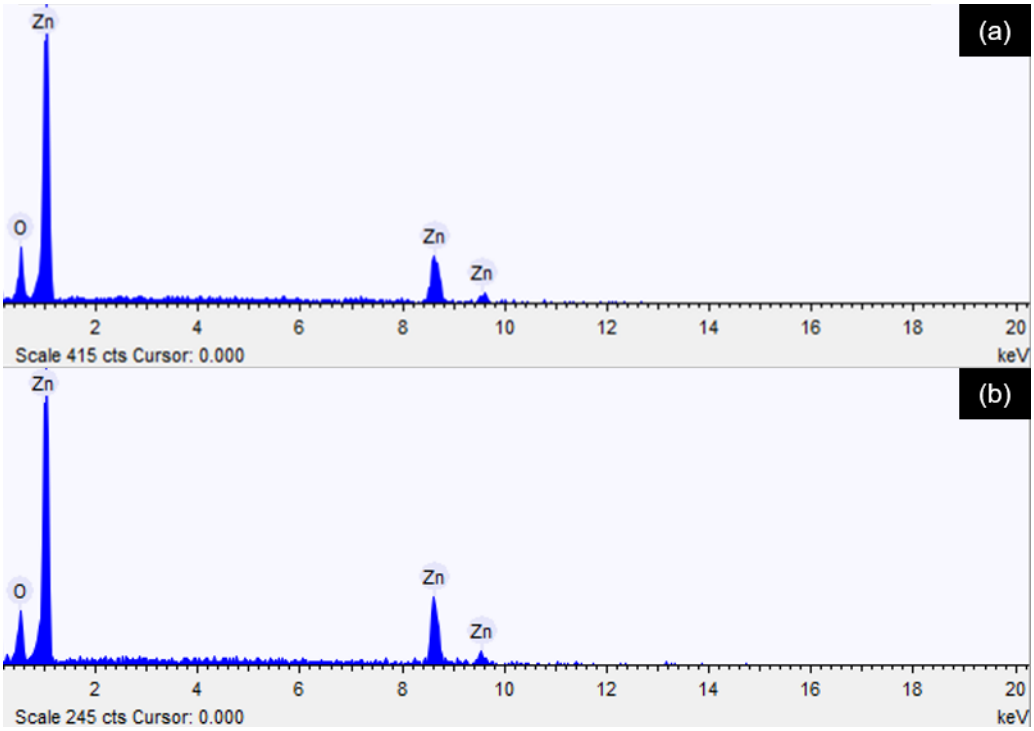

Figure 4 EDX spectrum of (a) Zno thin film and (b) Zno nanorods

Table 2: Elemental composition of zinc and oxygen in ZnO samples

Photoanode	Element	Weight %	Weight % σ	Atomic %
ZnO Thin Film	Oxygen	19.087	1.625	49.079
	Zinc	80.913	1.625	50.921
ZnO Nanorods	Oxygen	19.523	2.084	49.780
	Zinc	80.477	2.084	50.220

The absorbance spectra of both samples were taken in order to evaluate the optical characteristics of the created ZnO thin film and ZnO nanorods. The UV spectra for ZnO nanorods and thin films in the wavelength range of 300 to 800 nm is shown in Fig. 5(a). The red shift in the ZnO nanorods' absorption edge from thin films is visible. This demonstrates that ZnO nanorods have a larger range of UV-visible light absorption than ZnO thin films (Joy et al., 2018).

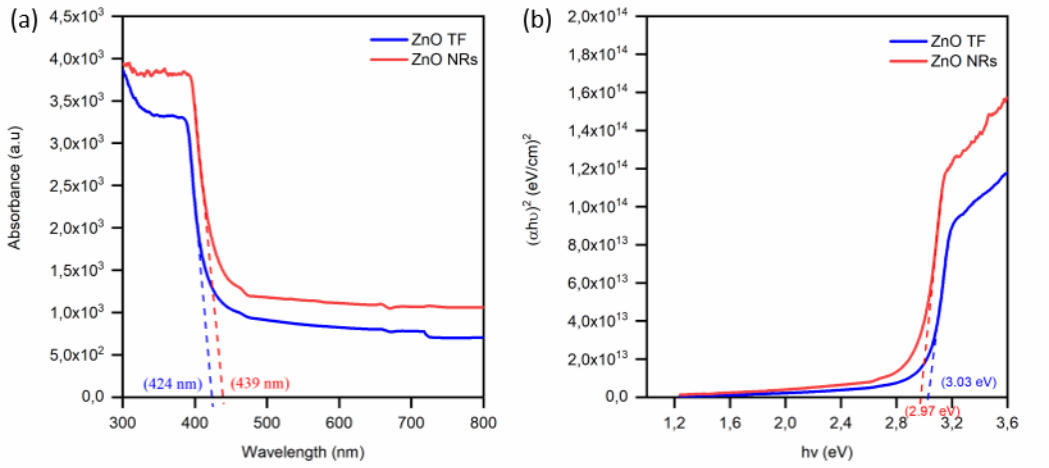

Figure 5 (a) Absorbance UV-Vis spectrum of ZnO thin film and nanorods; (b) Tauc plot of ZnO thin film and nanorods

Equation 2 can be used to determine the ZnO nanorods and thin films that have been fabricated to have direct optical band gaps:

$$(\alpha h\upsilon)^2 = A(h\upsilon - Eg)^n \quad (2)$$

Where A is a constant, υ is the frequency of the light, h is Planck's constant, Eg is the band gap energy, is the absorption coefficient and n is a parameter based on the band gap type, which was calculated to be 1/2 in this case. The band gap energy for a ZnO thin film was determined by plotting $(\alpha h\upsilon)^2$ versus $h\upsilon$, as seen in Figure 5(b). ZnO nanorods, on the other hand, have a narrower bandgap at 2.97 eV. The ZnO nanostructures may be the cause for the observed decrease in the band gap value of ZnO nanorods compared to ZnO thin film (Joy et al., 2018).

By graphing the current density (J) vs external bias voltage (V) relationship, the photoelectrochemical behaviour of both ZnO thin films and nanorods was examined. Figure 6 displays the J-V plot for ZnO thin films and nanorods in 1.0M NaOH in the dark and under 100 mW/cm^2 UV light irradiation. Additionally, Figure 6(a) and (b) demonstrate how the photoanodes' photocurrent density increased for both samples when they were exposed to light irradiation. In addition, ZnO nanorods have a greater photocurrent than ZnO thin film. This demonstrates how nanostructures, such nanorods, can increase photocurrent density (Joy et al., 2018).

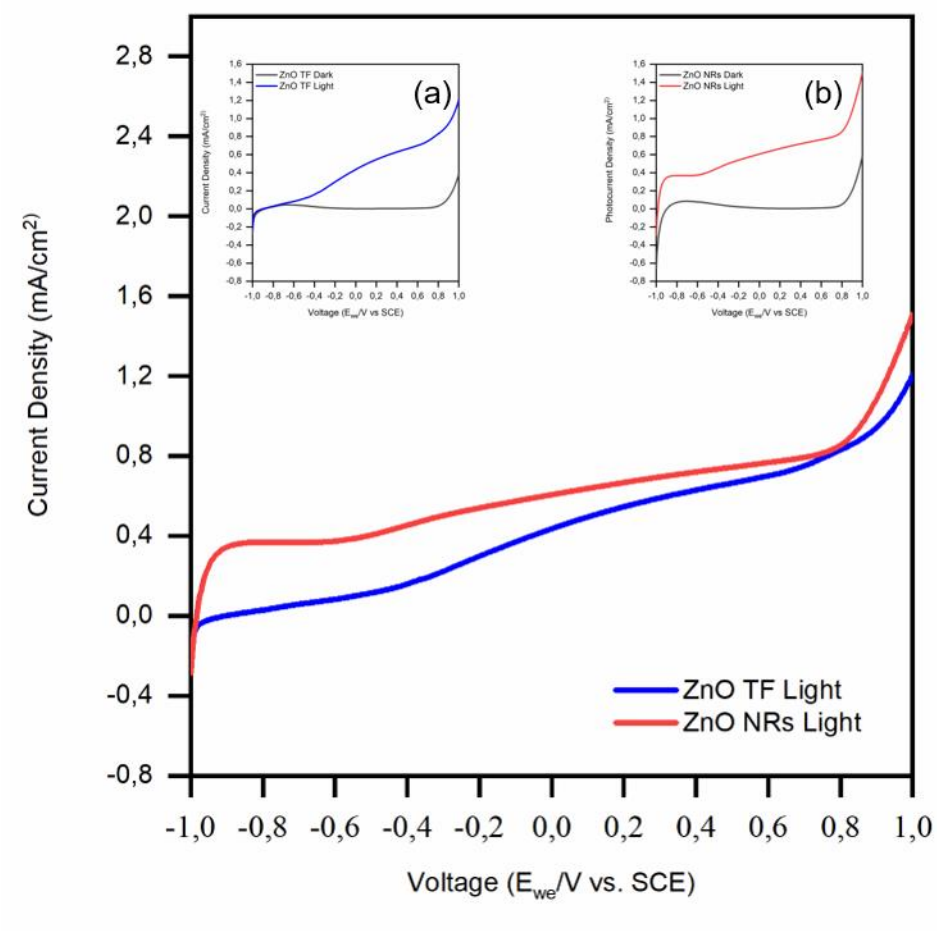

Figure 6 Current density (J) versus voltage (V) of ZnO thin film and ZnO nanorods with light irradiation. (a) ZnO thin film sample at dark and with light irradiation; (b) ZnO nanorods sample at dark and with light irradiation

Figure 7 depicts the ZnO thin film and nanorods' photoresponse to an on/off light irradiation cycle. Due to the temporary influence of the photon-generated carrier, which continuing in stable state during the light on, a spike in the photoresponse is seen for both samples under illumination. Additionally, when the light is turned off, the current rapidly decreases, showing a rapid transfer of charge carriers at the electrode/electrolyte interface (Jia et al., 2018).

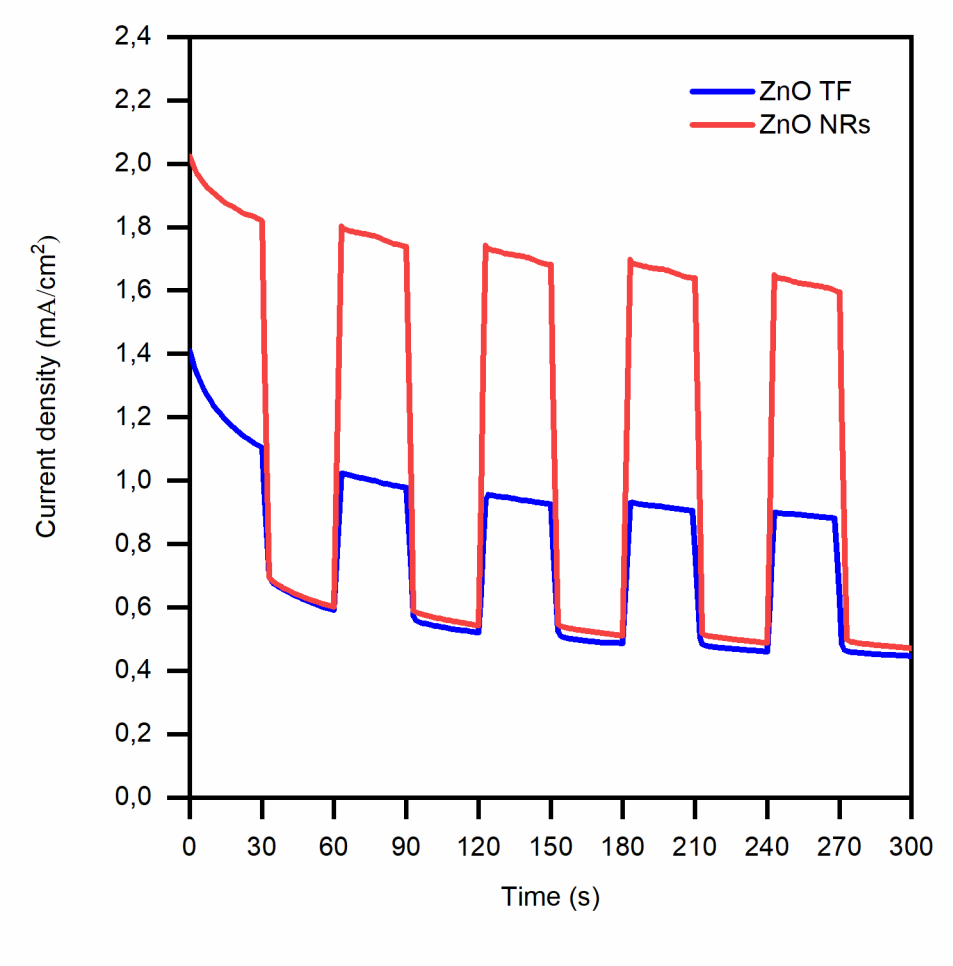

Figure 7 Current density (J) versus time (t) of ZnO thin film and nanorods at 1.0 V_{SCE}

Conclusion

In conclusion, homogeneous ZnO thin films and nanorods with narrow wall diameter were effectively fabricated on FTO substrates using spray pyrolysis and the sol-gel immersion approach, serving as a reliable photoanode for PEC water splitting. Using electrochemical, optical, and material characterization techniques, the photoelectrochemical and structural characteristics of the ZnO thin film and nanorods were examined. According to XRD, the structure of the manufactured nanorods at the (002) plane has changed compared to the ZnO thin film, which is required for improving the PEC water splitting system. Moreover, the hexagonal wurtzite ZnO was successfully synthesised, as proved by the FESEM images of ZnO nanorods. In agreement with a band gap of 2.97 eV, the absorbance spectra showed a high absorption edge of ZnO nanorods at about 439 nm, which supported the feasibility of modifying the band gap of ZnO photoanode by switching the structure from thin film to nanorods. Astonishingly, the ZnO nanorods' excellent photocurrent density (1.3 mA/cm^2 at 1.0 V_{SCE}) and quick photoresponse—with time rise and decay at about 3 seconds and photocurrent density difference at dark and light irradiation at around 1.2 to 1.3 mA/cm^2—show enhancement to the material's photocatalytic behaviour. Therefore, we anticipate that this research will pave the way for the creation and advancement of ZnO photoanodes to improve the PEC water splitting system.

Acknowledgement

This work is financially supported by International Matching Grant between Universiti Teknologi Malaysia and Universitas Negeri Malang Indonesia with cost center numbers of R.J130000.7354.4B685 and Q.J130000.3054.03M44.

References

Acar, C., & Dincer, I. (2014). Analysis and assessment of a continuous-type hybrid photoelectrochemical system for hydrogen production. *International Journal of Hydrogen Energy*, *39*(28), 15362–15372.

Dong, J., Zhao, Y., Shi, J., Wei, H., Xiao, J., Xu, X., Luo, J., Xu, J., Li, D., Luo, Y., & Meng, Q. (2014). Impressive enhancement in the cell performance of ZnO nanorod-based perovskite solar cells with Al-doped ZnO interfacial modification. *Chemical Communications*, *50*(87), 13381–13384.

Gu, P., Zhu, X., & Yang, D. (2020). Vertically aligned ZnO nanorods arrays grown by chemical bath deposition for ultraviolet photodetectors with high response performance. *Journal of Alloys and Compounds*, *815*, 152346.

Hassanpour, A., Bogdan, N., Capobianco, J. A., & Bianucci, P. (2017). Hydrothermal selective growth of low aspect ratio isolated ZnO nanorods. *Materials and Design*, *119*, 464–469.

Hsieh, P. Y., Wu, J. Y., Chang, T. F. M., Chen, C. Y., Sone, M., & Hsu, Y. J. (2020). Near infrared-driven photoelectrochemical water splitting: Review and future prospects. *Arabian Journal of Chemistry*, *13*(11), 8372–8387.

Inayat, A., Tariq, R., Khan, Z., Ghenai, C., Kamil, M., Jamil, F., & Shanableh, A. (2020). A comprehensive review on advanced thermochemical processes for bio-hydrogen production via microwave and plasma technologies. *Biomass Conversion and Biorefinery*.

Jia, G., Liu, L., Zhang, L., Zhang, D., Wang, Y., Cui, X., & Zheng, W. (2018). 1D alignment of ZnO@ZIF-8/67 nanorod arrays for visible-light-driven photoelectrochemical water splitting. *Applied Surface Science*, *448*, 254–260.

Joy, J., Mathew, J., & George, S. C. (2018). Nanomaterials for photoelectrochemical water splitting – review. *International Journal of Hydrogen Energy*, *43*(10), 4804–4817.

Kang, Z., Yan, X., Wang, Y., Bai, Z., Liu, Y., Zhang, Z., Lin, P., Zhang, X., Yuan, H., Zhang, X., & Zhang, Y. (2015). Electronic Structure Engineering of Cu 2 O Film/ZnO Nanorods Array All-Oxide p-n Heterostructure for Enhanced Photoelectrochemical Property and Self-powered Biosensing Application. *Scientific Reports*, *5*, 1–7.

Liu, Y., Yan, X., Kang, Z., Li, Y., Shen, Y., Sun, Y., Wang, L., & Zhang, Y. (2016). Synergistic Effect of Surface Plasmonic particles and Surface Passivation layer on ZnO Nanorods Array for Improved Photoelectrochemical Water Splitting. *Scientific Reports*, *6*(February), 1–7.

Mamat, M. H., Khusaimi, Z., Zahidi, M. M., Bakar, S. A., Siran, Y. M., Rejab, S. A. M., Asis, A. J., Tahiruddin, S., Abdullah, S., & Mahmood, M. R. (2011). Controllable growth of vertically aligned aluminum-doped zinc oxide nanorod arrays by sonicated sol-gel immersion method depending on precursor solution volumes. *Japanese Journal of Applied Physics*, *50*(6 PART 2), 10–15.

Nandi, R., Appani, S. K., & Major, S. S. (2016). Vertically aligned ZnO nanorods of high crystalline and optical quality grown by dc reactive sputtering. *Materials Research Express*, *3*(9), 1–10.

Nandi, R., & Major, S. S. (2017). The mechanism of growth of ZnO nanorods by reactive sputtering. *Applied Surface Science*, *399*, 305–312.

Ocakoglu, K., Mansour, S. A., Yildirimcan, S., Al-Ghamdi, A. A., El-Tantawy, F., & Yakuphanoglu, F. (2015). Microwave-assisted hydrothermal synthesis and characterization of ZnO nanorods. *Spectrochimica Acta - Part A: Molecular and Biomolecular Spectroscopy*, *148*, 362–368.

Ong, C. B., Ng, L. Y., & Mohammad, A. W. (2018). A review of ZnO nanoparticles as solar photocatalysts: Synthesis, mechanisms and applications. *Renewable and Sustainable Energy Reviews*, *81*(August 2017), 536–551.

Safwan, M., Aziz, A., & Shahril, M. (2022). *Structural , Morphological and Optical Properties of Zinc Oxide Nanorods prepared by ZnO Seed Layer Annealed at Different Oxidation Temperature*. *18*, 383–392.